Scientific Research Publishing

Open Journal of Medicinal Chemistry, 2026, 16(1), 1-14
https://www.scirp.org/journal/ojmc
ISSN Online: 2164-313X
ISSN Print: 2164-3121

Hemibastadin Alkaloid Analogues as Potential Anti-Biofilm Leads against Multi-Species Biofilms

Alain Kacou[1,2], Ange-Désiré Yapi[2], Yves Blache[1]

[1]MAPIEM, Université de Toulon, Toulon, France
[2]Unité Pédagogique de Chimie Thérapeutique-Chimie Organique, UFR Sciences Pharmaceutiques et Biologiques, Université Félix Houphouët-Boigny, Abidjan, Côte d'Ivoire
Email: akakacou@gmail.com

How to cite this paper: Kacou, A., Yapi, A.-D. and Blache, Y. (2026) Hemibastadin Alkaloid Analogues as Potential Anti-Biofilm Leads against Multi-Species Biofilms. *Open Journal of Medicinal Chemistry*, **16**, 1-14.
https://doi.org/10.4236/ojmc.2026.161001

Received: December 31, 2025
Accepted: January 26, 2026
Published: January 29, 2026

Abstract

A focused library of hemibastadin-inspired analogues was generated through a modular click chemistry strategy to assess their potential as antibiofilm agents targeting marine multispecies bacterial communities. The resulting triazole-amide derivatives **(4a-h)** were evaluated for their ability to inhibit initial bacterial adhesion and subsequent biofilm development in three Gram-negative strains. Clear structure-activity relationships emerged, highlighting the critical influence of aromatic bromination and methylation patterns on biofilm inhibition. Among the series, compounds **4g** and **4h** exhibited the most pronounced activity, with **EC_{50} values of 25 - 90 µM**, while exerting minimal effects on planktonic bacterial growth. Their potency was further confirmed in an original multispecies biofilm model, where both analogues achieved near-complete suppression of biofilm formation without detectable cytotoxicity, except toward a single more sensitive strain. Taken together, these findings identify **4g and 4h** as promising nontoxic leads for the development of cobiocidal or coantibiotic strategies aimed at preventing persistent biofilms on medical or industrial surfaces. The modularity of the synthetic route and the clear SAR trends provide a solid foundation for future optimization.

Keywords

Hemibastadin, Biofouling, Antibiofilm, Multi-Species Biofilm

1. Introduction

Biofouling is defined as the rapid colonization of microorganisms (bacteria,

microalgae, etc.) on living or artificial surfaces, causing health risks and significant economic damage in industrial or marine environments [1]-[3]. Any surface of human interest can serve as a starting ground for biofilm development, and although the control of the development of planktonic bacterial communities is well known and mastered, bacteria within a biofilm are much more resistant to antibiotics and/or biocides (up to 1000-fold increased resistance). In this context, the development of original compounds that specifically target biofilm formation is greatly needed in view of the rational use of antibiotics and/or biocides. Such biofilm inhibitors should have the potential to be used as a preventive treatment on a wide diversity of medical and/or industrial surfaces.

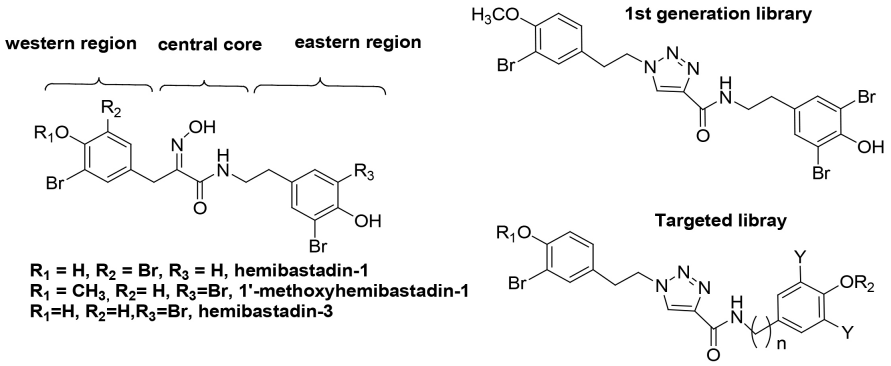

Figure 1. General structure of hemibastadins, a representative example of the 1st generation, and the structure of targeted compounds.

Some of the anti-biofilm techniques that are tested today are bioinspired by the observation of sessile marine macroorganisms such as sponges, corals, or macroalgae [1]-[4]. These species are constantly exposed to undesirable bacterial colonization (e.g., biofouling) and can maintain unfouled exterior surfaces with their arsenal of secondary metabolites possessing antifouling properties [5]-[7]. However, these natural products are only obtained in small quantities, are generally toxic, and are not stable over time [8]-[19]. In this context and in a biomimetic approach, our previous preliminary investigations aimed at the discovery of new bioactive compounds showed that bromotyrosine analogues possessing a central triazole ring were good candidates as antibiofilm compounds [20] [21]. Among all classes studied, we found that hemibastadin analogues possessing a central 1,2,3-triazolic ring were the most potent (**Figure 1**). Conjugation of the western moiety to the eastern moiety was assumed through the triazole core. This could be achieved by a click reaction according to the copper (I)-catalyzed 1,3-dipolar cycloaddition of organic azides and alkynes, leading to the formation of 1,4-disubstituted 1,2,3-triazoles [22]. This methodology was attractive because it is a highly efficient process in bond formations among diverse building blocks that usually proceeds in 6 - 36 h at ambient temperature in water with a variety of organic co-solvents (tert-butanol, ethanol, DMSO, THF, or CH_3CN) [22] [23]. Pursuing these investigations, we are now interested in the advanced SAR studies

of hemibastadin derivatives, and we wish to report here the synthesis and biological results of an advanced library of hemibastadin analogues as potential antibiofilm compounds on different marine bacterial strains, and validation of their efficiency with an original model of multi-species biofilm.

2. Experimental Section

2.1. Chemistry

Preparation of intermediary carboxylic acids **3a, 3b** was performed according to the methodology described in our previous reports [20] [21]. These compounds were obtained in excellent yield in two steps. Treatment of halogeno compounds **1a, 1b** with sodium azide in dimethylformamide afforded the corresponding azides **2a** and **2b**. Synthesis of the targeted carboxylic acids **3a** and **3b** was then achieved by performing the copper (I)-catalyzed 1,3-dipolar cycloaddition of the organic azides with propargylic acid, resulting in the formation of 1,2,3-triazoles. Ethanol was chosen as a co-solvent to allow an easier workup and better purity of products as in our previous work [17]. In practice, propargylic acid was added at room temperature to a solution of the appropriate azide **2a, 2b**, $CuSO_4$/sodium ascorbate in a water/ethanol mixture (50/50), and the reaction time was optimized at 12 hours at room temperature. Access to the different bromotyramine analogues **4a-h** was then achieved by a peptide coupling step using EDC/HOBt methodology [22]. All amides were obtained in good yields. Scheme 1 summarizes the different steps involved in the preparation of the amides.

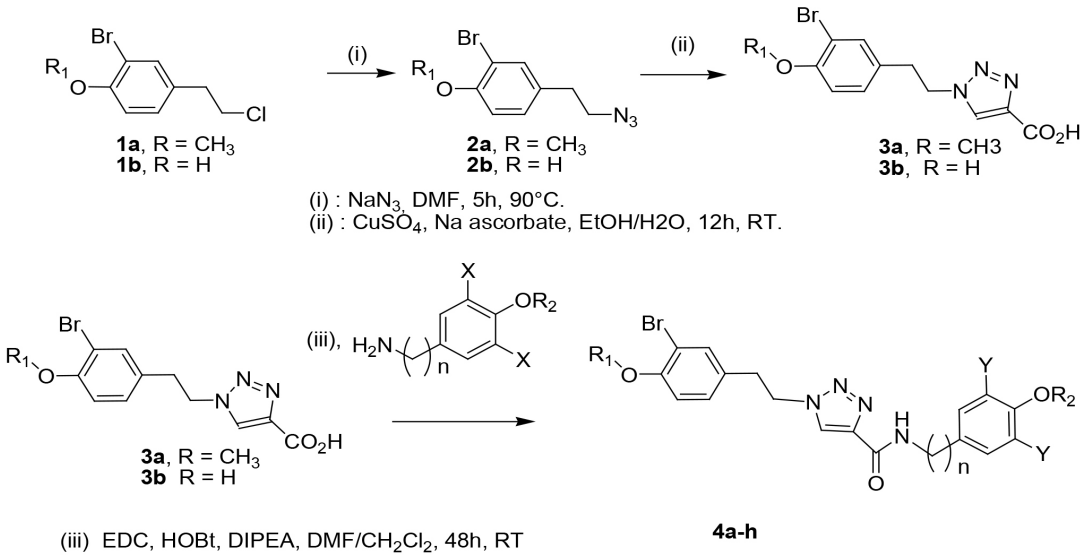

Scheme 1. Synthesis of hemibastadin analogues.

General Methods: All commercially available chemicals and reagents were used without any further purification. ^{1}H and ^{13}C NMR spectra were recorded at 400 and 100 MHz, respectively, on a Brüker Avance 400 MHz spectrometer. The spectra were recorded in $CDCl_3$ and D6-acetone as solvents. Multiplicity was

indicated as follows: s (singlet); d (doublet); t (triplet); m (multiplet); dd (doublet of doublets), etc. Coupling constants (*J*) were given in Hz. Chemical shifts are reported in δ relative to TMS as an internal standard. Mass spectra were measured on an ion trap mass spectrometer fitted with an ESI interface (Esquire 6000, Brüker Daltonics).

Typical procedure for the preparation of azides **2a, 2b**

A mixture of the appropriate halide (1 equiv) and NaN_3 (2.6 equiv) in DMF was stirred for 5 h at 90˚C. The reaction temperature was then allowed to warm to room temperature, and the reaction mixture was diluted with Et_2O. The organic phase was washed with brine and water, dried over Na_2SO_4, and concentrated under vacuum. The azide products were directly used for the next reaction without further purification.

Typical procedure for preparation of triazoles **3a, 3b**

Appropriate azide (1 equiv.) and propiolic acid (1.5 equiv.) were dissolved in a 1:2 mixture of water and EtOH. To this was added $CuSO_4$. $5H_2O$ (0.04 equiv.) and sodium ascorbate (0.08 equiv.). The resultant mixture was stirred at room temperature for 12 h, at which time TLC revealed complete conversion. The reaction solution was diluted with water and extracted three times with $CHCl_3$. The reaction solution was diluted with brine and extracted three times with EtOAc. The organic layers were washed with water, dried over Na_2SO_4, and evaporated under vacuum. Crude triazoles were purified by silica gel column chromatography using a mixture of EtOAc/cyclohexane as the mobile phase.

Typical procedure for preparation of amide compounds **4a-h**

To a stirred solution of the acid (1.28 mmol) in CH_2Cl_2/MeOH (9 ml/1ml), 1-Ethyl-3-(3-dimethylaminopropyl)-carbodiimide (1.2 eq) and Hydroxybenzotriazole (1.2 eq) were added. The mixture was stirred at room temperature under nitrogen for 5 min, and the appropriate amine (1 eq) and diisopropylethylamine (100 µL) were added. The reaction was stirred at room temperature for 48 hours. A saturated NaCl solution was added and the organic layer was extracted three times with CH_2Cl_2. The solvent was removed in vacuo and the residue was purified by flash chromatography (SiO_2) using CH_2Cl_2/MeOH as eluent to yield compounds.

2.2. Biology

Bacterial strains

Six marine Gram-negative bacterial strains *Pseudoalteromonas ulvae* (TC14), *Pseudoalteromonas lipolytica* (TC8), *Paracoccus* sp. (4M6), *Persicivirga* (*Nonlabens*) *mediterranea* TC4, *Shewanella* sp. TC10, and *Shewanella* sp. TC11 [23].

TC14 was isolated in June 2010 in Little Bay of Toulon (1 m depth, Mediterranean Sea, France) [23]. The strain 4M6 was provided by the LBCM (Université de Bretagne Sud). It was isolated on glass slides immersed for 6 h at 1 m depth in March 2000 in the Morbihan Gulf (Bailleron Island, 47_3403700N-2_4405400W, Atlantic Ocean) [24]. TC8 was isolated in February 2008 in Little Bay of Toulon (1 m

depth, Mediterranean Sea, France) [25]. TC4, TC10, and TC11 have also been isolated from various surfaces immersed in Little Bay of Toulon (1 m depth, Mediterranean Sea, France). TC10 harbored the pX5 plasmid encoding GFP (constructed by Dr. Aurore Puymège).

Anti-adhesion bioassays: [23]

Bacterial strains were grown on Väätänen Nine-Salts Solution (VNSS). When the stationary phase was reached, the bacterial suspension was centrifuged. Cells were then diluted in sterile artificial sea water (ASW) and introduced into microtiter plates (sterile black PS; Nunc, Fisher Scientific, France) with tested molecules at eight concentrations (2, 5, 10, 20, 50, 100, 150, and 200 µM) in three replicates in the presence of three controls: 1) non-specific staining control, 2) adhesion control, and 3) positive control. The maximum percentage of solvent (final concentration = DMSO 2%) used for the dilution of biocides was also tested in triplicate as an additional control. After incubation during an optimized adhesion time (approximately 15 h), the non-adhered bacteria were eliminated and the adhered cells were quantified after SYTO® 61 (Molecular Probes® Invitrogen, France) (1 µM) staining. A percent of inhibition was calculated per well:

$$(\text{Mean FIi} - \text{nsCi})/(\text{Mean Fic} - \text{Mean B}) \times 100$$

with FIi as the fluorescence intensity in a treated well (tested compound + bacteria + SYTO® 61), FIc as the fluorescence intensity in a control well (bacteria + SYTO® 61), nsCi as the nonspecific control (tested compound without bacteria + SYTO® 61), and B as the blank, *i.e.*, stain control (only SYTO® 61). A sigmoid dose–response curve was obtained when the percentage of inhibition was plotted with the log of compound concentrations, after calculation of the mean (n = 3) and standard deviation (SD) per triplicate for each concentration. EC_{50} values were then calculated for each compound using GraphPad Prism® (GraphPad Software, USA). This software also allowed the performance of statistical tests dedicated to the analysis of two variables simultaneously, such as the difference between strains and between biocides (two-way ANOVA). Significant differences were accepted when $p < 0.05$.

Toxicity tests: [25]

After growth on VNSS, bacterial strains were picked up during the exponential phase. The microtiter plates (sterile transparent PS) were filled as described in the protocol of the antiadhesion assay but using VNSS instead of ASW to allow bacterial growth. The bacterial growth was monitored by measuring the turbidity (OD_{600nm}) every hour for 7 hours. Then, resazurin (50 µM) was added to all the wells, and fluorescence was measured after 2 h to quantify the percent of bacterial viability. The same methodology used with SYTO® 61 was applied to calculate the percent of viability after resazurin staining. Only compounds with EC_{50} lower than 200 µM were tested, and experiments were performed at a concentration of 100 µM of each compound using ethanol 50% as a positive antibacterial reference.

Multispecies biofilm formation

This test using TC4, TC11, and TC10 was conducted by strictly following the procedure previously described in the MAPIEM laboratory [26] [27].

Bacterial labelling: This was performed with TC4, TC11, and TC10. TC10-pX5-GFP was obtained by conjugation using *E. coli* WM3064 as a 113 donor strain. Briefly, post-exponential phase culture of WM3064 transformed with pX5-GFP 114 was mated with post-exponential phase *Shewanella* sp. TC10 in a 1:1 ratio on VNSS plates 115 containing 100 µg/ml of DAP (2,6-diaminopimelic acid) (Sigma-Aldrich, Saint Louis, 116 Missouri, USA) overnight at 20˚C. *Shewanella* sp. TC10 transconjugants were selected on 117 VNSS DAP-free agar plates containing 6 µg/mL of chloramphenicol.

Anti-multispecies biofilm assay: To test the capability of the molecule to inhibit multispecies biofilm, this test was conducted with three species: TC4, TC11, and TC10-pX5-GFP on a 24 h biofilm. After growth in VNSS, bacteria in the post-exponential growth phase were suspended in ASW and inoculated into 24-well plates (Corning Incorporated Costar®) containing a sterilized glass coverslip in each well to a final OD_{600nm} of 0.3 (0.1 per strain). This test was performed with and without 100 µM of the molecule previously determined to be the most effective. Controls included single-species biofilms formed under the same conditions. After 24 h, cells were fixed using 3.7% Formalin for 15 min. For the immunostaining, samples were blocked with 3% BSA (Acros Organics, Gelle, Belgium) in PBS 1X overnight at 4˚C. The primary antibodies were added for 1h in 190 BSA 3% at 1/300 for Chicken-anti-TC4, 1/100 for Goat-anti-TC5, and 1/300 for Rabbit-anti-191 TC11. After a second blocking step of 2h at room temperature, the secondary antibodies were 192 added in BSA 3% to a concentration of 1/2000 for Goat anti-Chicken IgY (H + L) conjugated to 193 FITC (Invitrogen™, Waltham, Massachusetts, USA) for 1h, to a concentration of 1/500 for 194 Goat anti-Chicken IgY (H + L) conjugated to Alexa Fluor 405 (Abcam, Cambridge, United 195 Kingdom) for 1h, to a concentration of 1/1000 for Donkey anti-Goat IgG (H + L) coupled to 196 Alexa Fluor 633 (Invitrogen™, Waltham, Massachusetts, USA) for 1h, to a concentration of 45 µL/mL for Donkey anti-Rabbit IgG coupled to Alexa Fluor 594 for 30 min and to a concentration of 1/200 for Mouse anti-rabbit IgG coupled to CruzFluor™ 488 for 1h. Finally, the coverslips were mounted with a drop of ProLong™ Diamond Antifade before observation 200 using CLSM.

Data Extraction From Images and Statistics

At least three replicates and five pictures per replicate were performed and used for data extraction. The pictures were acquired by CLSM. The biovolume was determined with the COMSTAT2 software [28] [29]. Results were obtained using automatic thresholding.

3. Results and Discussion

3.1. Chemistry

Structures of the obtained compounds are summarized in **Table 1**.

Table 1. Selected 1,4-disubstituted 1,2,3-triazoles.

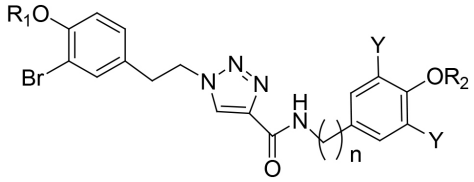

n	R1	R2	X	Compound (yield)*
0	H	CH3	H	4a (65%)
0	CH3	CH3	H	4b (73%)
0	H	H	H	4c (68%)
1	H	CH3	H	4d (78%)
1	CH3	CH3	H	4e (85%)
1	H	H	H	4f (57%)
1	H	H	Br	4g (85%)
2	H	H	Br	4h (88%)

*yield of peptide coupling step (EDC/HOBt).

1-(3-bromo-4-hydroxyphenethyl)-N-(4-methoxyphenyl)-1H-1,2,3-triazole-4-carboxamide (4a)

This compound was obtained from acid (**2**) and p-anisidine as a white solid (65%). mp 214˚C - 216˚C.

^{1}H NMR (400 MHz, DMSO-d_6) δ 10.30 (s, 1H), 10.10 (s, 1H), 8.61 (s, 1H), 7.72 (d, J = 8.9 Hz, 2H), 7.35 (s, 1H), 6.96 (s, 1H), 6.93 (d, J = 8.2, 1H), 6.84 (d, J = 8.5 Hz, 2H), 4.66 (t, J = 7.1 Hz, 2H), 3.74 (s, 3H), 3.11 (t, J = 7.1 Hz, 2H). ^{13}C NMR (100 MHz, DMSO-D_6) δ 158.3, 154.5, 149.8, 143.4, 133.5, 131.51, 130.50, 129.7, 127.6, 122.6 (2C), 115.4 (2C), 112.9, 111.2, 56.57, 51.2, 34.5. Found MS (ESI, *m*/*z*) for $C_{18}H_{17}N_4O_3Br$: $[M + H]^+$, 416.84 $[M + H + 2]^+$, 418.84.

1-(3-bromo-4-methoxyphenethyl)-N-(4-methoxyphenyl)-1H-1,2,3-triazole-4-carboxamide (4b)

This compound was obtained from acid (**1**) and p-anisidine as a brown solid (73%). mp > 250˚C.

^{1}H NMR (400 MHz, DMSO-D_6) δ 10.30 (s, 1H), 8.64 (s, 1H), 7.72 (d, J = 9.1 Hz, 2H), 7.49 (s, 1H), 7.14 (d, J = 8.3 Hz, 1H), 7.01 (d, J = 8.5 Hz, 1H), 6.91 (d, J = 9.1 Hz, 2H), 4.69 (t, J = 7.2 Hz, 2H), 3.8 (s, 3H), 3.74 (s, 3H), 3.17 (t, J = 7.2 Hz, 2H). ^{13}C NMR (100 MHz, DMSO-D_6) δ 158.3, 154.2, 153.3, 143.4, 133.3, 130.5, 129.9 (2C), 127.4, 122.6, 116.7 (2C), 115.4, 109.6, 55.7, 51.3, 49.06, 34.7. Found MS (ESI, *m*/*z*) for $C_{19}H_{19}N_4O_3Br$: 430.87 $[M + H]^+$, 432.87 $[M + H + 2]^+$.

1-(3-bromo-4-hydroxyphenethyl)-N-(4-hydroxyphenyl)-1H-1,2,3-triazole-4-carboxamide (4c)

This compound was obtained from acid (2) and 4-aminophenol as a brown solid (68%). mp > 250˚C.

^{1}H NMR (400 MHz, DMSO-D_6) δ 10.17 (s, 1H), 10.10 (s, 1H), 9.24 (s, 1H), 8.59 (s, 1H), 7.57 (d, J = 8.9 Hz, 1H), 7.37 (s, 1H), 6.96 (d, J = 8.3 Hz, 1H), 7.01 (d, J = 8.5 Hz, 1H), 6.72 (d, J = 8.9 Hz, 2H), 4.68 (t, J = 7.1 Hz, 2H), 3.16 (t, J = 7.1 Hz,

2H). ^{13}C NMR (100 MHz, DMSO-D_6) δ 158.3, 154.2, 153.3, 143.4, 133.3, 130.5, 129.9 (2C), 127.4, 122.6, 116.7 (2C), 115.4, 109.6, 51.3, 34.7. Found MS (ESI, *m*/*z*) 403.02 $[M + H]^+$, 405.02 $[M + H + 2]^+$.

1-(3-bromo-4-hydroxyphenethyl)-N-(4-methoxybenzyl)-1H-1,2,3-triazole-4-carboxamide (4d)

This compound was obtained from acid (**2**) and 4-methoxybenzylamine as a white solid (78%). mp 162˚C - 164˚C.

^{1}H NMR (400 MHz, DMSO-d_6): δ 10.10 (s, 1H, OH), 8.97 (t, J = 6.2 Hz, 1H, NHCO), 8.48 (s, 1H), 7.33 (d, J = 2.1 Hz, 1H), 7.24 (d, J = 8.7 Hz, 1H), 6.95 (dd, J = 8.3 Hz, 1H), 6.87 (d, J = 8.7 Hz, 1H), 6.83 (d, J = 8.2 Hz, 1H), 4.61 (t, J = 7.1 Hz, 2H), 4.36 (d, J = 6.2 Hz, 2H), 3.72 (s, 3H), 3.08 (t, J = 7.1 Hz, 2H). ^{13}C NMR (100 MHz, DMSO-D_6) δ 159.9, 156.6, 153.1, 143.1, 133.3, 132.1, 129.9, 129.4, 129.1 (2C), 126.8, 116.6, 114.1 (2C), 109.6, 55.5, 51.2, 41.8, 34.6. Found MS (ESI, *m*/*z*) for $C_{19}H_{19}N_4O_3Br$: 431.03 $[M + H]^+$, 433.02 $[M + H + 2]^+$.

1-(3-bromo-4-methoxyphenethyl)-N-(4-methoxybenzyl)-1H-1,2,3-triazole-4-carboxamide (4e)

This compound was obtained from acid (**1**) and 4-methoxybenzylamine (85%). mp 141˚C - 143˚C.

^{1}H NMR (400 MHz, DMSO-d_6) δ 8.98 (t, J = 6.3 Hz, 1H, NHCO), 8.5 (s, 1H), 7.45 (s, 1H), 7.23 (d, J = 6.3 Hz, 2H), 7.11 (s, 1H), 7.00 (d, J = 8.5 Hz, 1H), 6.87 (d, J = 8.7 Hz, 2H), 4.64 (t, J = 7.1 Hz, 2H), 4.34 (d, J = 6.2 Hz, 2H), 3.79 (s, 3H), 3.72 (s, 3H), 3.13 (t, J = 7.1 Hz, 2H). ^{13}C NMR (100 MHz, DMSO-D_6) δ 158.7, 154.7, 143.3, 133.4, 132.2, 131.6, 130.2, 129.8 (2C), 129.2, 126.9, 114.16 (2C), 113.07, 110.9, 56.6, 55.6, 51.2, 41.8, 34.5. Found MS (ESI, *m*/*z*) for $C_{20}H_{21}N_4O_3Br$: 445.12 $[M + H]^+$, 447.12 $[M + H + 2]^+$.

1-(3-bromo-4-hydroxyphenethyl)-N-(4-hydroxybenzyl)-1H-1,2,3-triazole-4-carboxamide (4f)

This compound was obtained from acid (2) and 4-hydroxybenzylamine (57%). mp 173˚C - 175˚C.

^{1}H NMR (400 MHz, DMSO-D_6) δ 10.08 (s, 1H, OH), 9.25 (s, 1H, OH), 8.88 (t, J = 6.3 Hz, 1H, NHCO), 8.47 (s, 1H), 7.34 (d, J = 2.1 Hz, 1H), 7.11 (d, J = 8.2 Hz, 1H), 6.94 (d, J = 8.3 Hz, 2H), 6.82 (d, J = 8.3, 1H), 6.69 (d, J = 8.3 Hz, 2H), 4.60 (t, J = 7.1 Hz, 2H), 4.31 (d, J = 5.6 Hz, 2H), 3.79 (s, 3H), 3.07 (t, J = 7.1 Hz, 4H). ^{13}C NMR (100 MHz, DMSO-D_6) δ 159.9, 156.6, 153.1, 143.1, 133.3, 130.2, 129.9, 129.4 (2C), 129.1, 126.8, 116.6 (2C), 115.4, 109.6, 51.2, 40.4, 34.6. Found MS (ESI, *m*/*z*) for $C_{18}H_{17}N_4O_3Br$: 417.01 $[M + H]^+$; 419.01 $[M + H + 2]^+$.

N-(3,5-dibromo-4-hydroxybenzyl)-1-(3-bromo-4-hydroxyphenethyl)-1H-1,2,3-triazole-4-carboxamide (4g)

This compound was obtained from acid (2) and 3,5-dibromo-4-hydroxybenzylamine (85%). mp 214˚C - 216˚C.

^{1}H NMR (400 MHz, DMSO-D_6) δ 10.09 (s, 1H, OH), 9.83 (s, 1H, OH), 9.10 (t, *J* = 6.3 Hz, 1H, NHCO), 8.50 (s, 1H), 7.47 (s, 1H), 7.31 (s, 1H), 6.96 (d, *J* = 7.8 Hz, 1H), 6.83 (d, *J*= 8.3, 1H), 4.61 (t, *J* = 7.2 Hz, 2H), 4.32 (d, *J* = 6.2 Hz, 2H), 3.07 (t,

J = 7.3 Hz, 2H). ^{13}C NMR (100 MHz, DMSO-D_6) δ160.2, 153.3, 150.1, 142.9, 133.5, 131.8, 130.0, 129.4, 127.0, 116.9, 112.2, 109.5, 79.6, 51.3, 34.5, 29.5. Found MS (ESI, *m*/*z*) for $C_{18}H_{15}N_4O_3Br_3$: 572.8 $[M + H]^+$, 574.8 $[M + H + 2]^+$.

1-(3-bromo-4-methoxyphenethyl)-N-(4-hydroxyphenethyl)-1H-1,2,3-triazole-4-carboxamide (4h)

This compound was obtained from acid (2) and 3,5-dibromotyramine (88%). mp 171˚C - 173˚C.

^{1}H NMR (400 MHz, DMSO-D_6) δ10.09 (s, 1H, OH), 9.83 (s, 1H, OH), 9.10 (t, *J* = 6.3 Hz, 1H, NHCO), 8.50 (s, 1H), 7.47 (s, 1H), 7.31 (s, 1H), 6.96 (d, *J* = 7.8 Hz, 1H), 6.83 (d, *J*= 8.3, 1H), 4.61 (t, *J* = 7.2 Hz, 2H), 4.32 (d, *J* = 6.2 Hz, 2H), 3.07 (t, *J* = 7.3 Hz, 2H). ^{13}C NMR (100 MHz, DMSO-D_6) δ162.8, 160.2, 149.3, 143.1, 134.4, 133.3, 132.6, 130.1, 129.4, 126.7, 116.7, 112.2, 109.5, 51.1, 36.2, 34.6, 33.5. Found MS (ESI, *m*/*z*) for $C_{19}H_{17}N_4O_3Br_3$: 586.89 $[M + H]^+$; 588.89, $[M + H + 2]^+$.

3.2. Antibiofilm Activity

Compounds **4a-h** were assessed for their antibiofilm activity against three strains of gram-negative bacteria (*Pseudoalteromonas ulvae* (TC14), *Pseudoalteromonas lipolytica* (TC8), *Paracoccus* sp. (4M6)) [25]. In an initial screening process, all compounds were tested for their ability to modulate biofilm formation at a concentration of 200 µM by using our previous method adapted from Leroy *et al.*, using the specific fluorophore Syto®61 [25] [30]. In order to clarify structure-activity relationships, effective concentrations to inhibit 50% of bacterial adhesion (expressed as EC_{50}) were determined for active compounds. Different elements were considered to obtain information about structure-activity relationships: length of the chain at the eastern region (n = 0, 1, 2), O-methylation on the aromatic rings, and finally, degree of bromination. Antibiofilm activities are summarized in Table 2 below.

Table 2. biological screening against bacterial biofilms of *Paracoccus sp.* (4M6), *Pseudoalteromonas lipolytica* (TC8), *Pseudoalteromonas ulvae* (TC14). Results are expressed as the effective concentration to inhibit 50% of biofilm formation (EC_{50}) in micromoles/L (µM). Data represent means ± standard deviation values from three independent experiments.

Compound	TC8		4M6		TC14	
	% *of adhesion*[a]	EC_{50}	% *of adhesion*	EC_{50}	% *of adhesion*	EC_{50}
4a	60.8 ± 14.4	>200	67.9 ± 5.9	>200	34.3 ± 3.3	65.2 ± 0.9
4b	ND	NT	ND	NT	ND	NT
4c	68.7 ± 10.7	>200	32.2 ±	79.0 ± 17.4	22.9 ± 16.1	90.6 ± 0.1
4d	55.5 ± 6.7	>200	44.2 ± 2.3	174.3 ± 18.0	32 .3 ± 8.2	88.2 ± 11.7
4e	ND	NT	ND	NT	ND	NT
4f	65.3 ± 5.4	>200	66.2± 5.3	>200	39.6 ± 1	156.0 ± 15.1
4g	14.1 ± 11.7	91.5 ± 27.0	44.2 ± 2.3	27.1 ± 4.9	15.1 ± 1.4	32.3 ± 1.2
4h	36.2 ± 5.3	60.4 ± 4.1	11.8 ± 2.6	28.8 ± 8.2	19.6 ± 11.6	26.7 ± 7.8
Ampicillin	NT	17.9 ± 1.0	NT	144.1 ± 0.6	NT	9.3 ± 1.0

a. Percentage of adhesion at 200 µM compared to untreated samples. ND: adhesion > 95%. NT not tested.

Results indicated that the degree of methylation was of primary relevance for

assessing the activity. The efficiency of compounds decreased when the two hydroxyl groups were methylated (**4b, 4e** when compared to **4a** and **4d**). On the other hand, it appeared that the degree of bromination of the eastern moiety (**4g, 4h**) was of primary importance in affording an interesting biological response as antibiofilm compounds, with EC_{50} ranging from 90 to 25 µM toward the different strains.

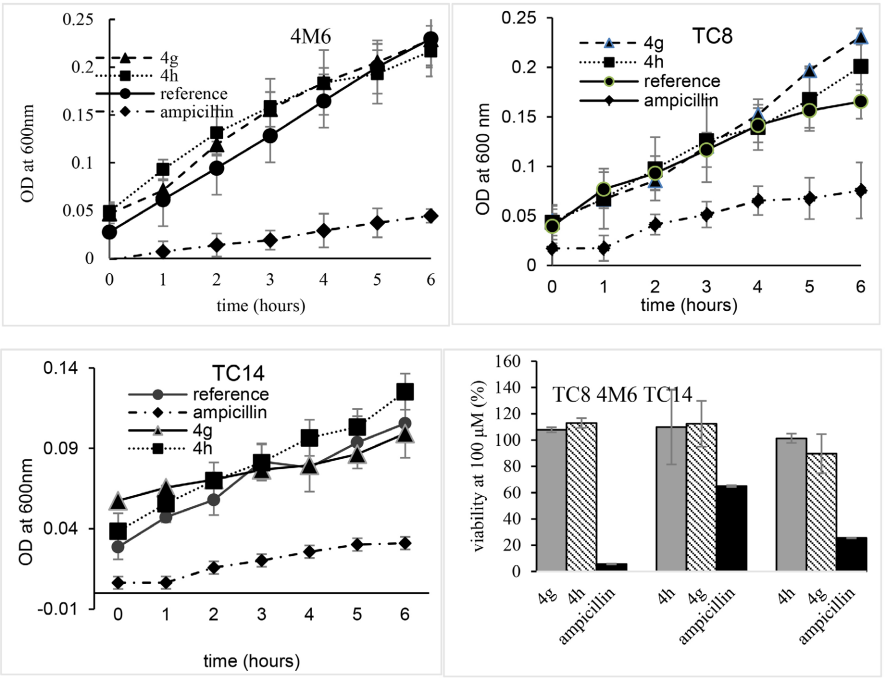

Figure 2. Effect of compounds 4g and 4h at a concentration of 100 µM on the bacterial growth of *Pseudoalteromonas lipolytica* TC8 (up, left), *Paracoccus* sp. 4M6 (up, right), *Pseudoalteromonas ulvae* TC14 (down, left). Results are expressed by measurement of optical density at 600 nm over 6 hours. Ampicillin (5 µM) was used as a bactericidal control, and an untreated sample was used as a positive reference. (Down, right): effect of compounds 4g and 4h at a concentration of 100 µM on the viability of the three strains. Data are expressed as % of viable bacteria when compared to an untreated sample with 100% viability. All values are the mean of three replicates.

In order to verify whether the compounds **4g** and **4h** exhibited specific antibiofilm activity or if this observation was simply related to a general toxic effect on the bacteria, a growth inhibition and viability assay was performed. Active compounds **4g** and **4h** were tested for their capacity to inhibit the growth of the three strains TC14, TC8, and 4M6 over 6 hours. Experiments were performed at the high concentration of 100 µM and using ampicillin at a concentration of 5 µM as a reference. We have already shown that the antibiofilm activity of ampicillin was directly connected to an antibacterial and general toxic effect on these different strains (especially against TC8 and TC14), but in contrast, the results presented in Figure 2 showed that when compared to untreated samples, the compounds **4g** and **4h** exhibit no effect on the bacterial growth of the TC14 strain. For viability,

the same methodology used for the antiadhesion assay with Syto®61 was applied using the resazurin test at the concentration of 100 µM.

This suggested that their anti-biofilm activities were not directly connected to antibacterial effect, in contrast to ampicillin, which is toxic especially towards TC14 and TC8. In regard to these results, and as most biofilm communities are composed of multiple different bacteria living in close proximity, compounds 4g and 4h, which were identified as the more potent and non-toxic compounds, were selected for a test against a multispecific biofilm. Such multispecies biofilms could be used as a routine model to test newer biocidal agents. For this purpose, we have developed a model of three bacterial species *Persicivirga* (Nonlabens) *mediterranea* TC4, *Shewanella* sp. TC10 and *Shewanella* sp. TC11 [23] [26]. In practice, a preliminary screening of toxicity of compounds 4g, 4h at a concentration of 100 µM showed no effect on growth and viability of TC10 and TC11 strains, while the TC4 strain was more sensitive to exposure to compounds 4g and 4h. Additionally, we can note that the known antibiotic ampicillin presented the same profile against TC4, while being less active on the two other strains (**Figure 3**).

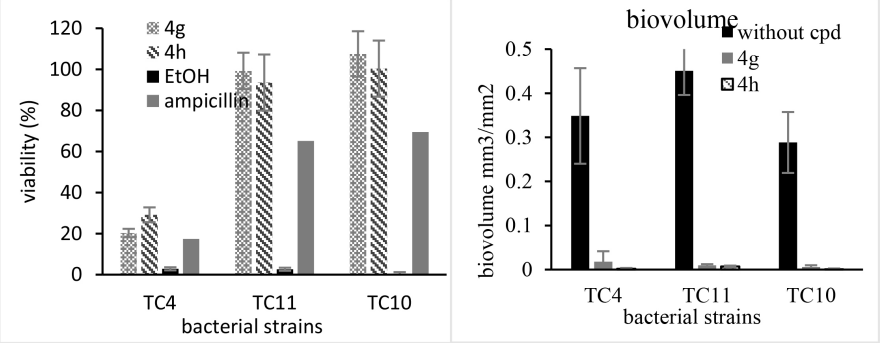

Figure 3. Left, effect of compounds **4g** and **4h** at a concentration of 100 µM on the viability of the 3 strains using ampicillin (5 µM) and ethanol as references. Data are expressed as % of viable bacteria compared to an untreated sample with 100% viability. All values are the mean of three replicates. Right, biovolumes measured at 24 h for each strain in three-species biofilms. Results report the untreated samples (black) and samples treated with compounds **4g** and **4h** at 100 µM (grey). All values are the mean of three replicates.

For the multispecies experiment, TC4, TC10, and TC11 were inoculated in the same proportion onto glass coverslips, and the biofilms were studied at 24 h using confocal laser scanning microscopy (CLSM). Experiments were conducted with compounds **4g** and **4h** at 100 µM and without compounds as a reference. **Figure 4** shows the CLSM pictures.

Measurement of the biovolumes of each strain within the multispecies biofilm with and without compounds **4g** and **4h** revealed that the two compounds reduced by around 100% the formation of the biofilm of the three strains. No significant differences can be noted between the results on TC4, for which **4g** and **4h** are toxic, with those observed for the two other strains. The results of this measurement are confirmed by examination of confocal laser scanning microscopy

images, which showed a total inhibition of the biofilm growth. Taken together, our results strongly indicate that compound **4g** and **4h** act as potent and specific antibiofilm agents against Gram-negative bacteria. Since the growth and viability of the different strains were poorly affected by exposure to the compounds (except TC4), we can consider them as non-toxic on the different isolated strains as well as on multispecies biofilms.

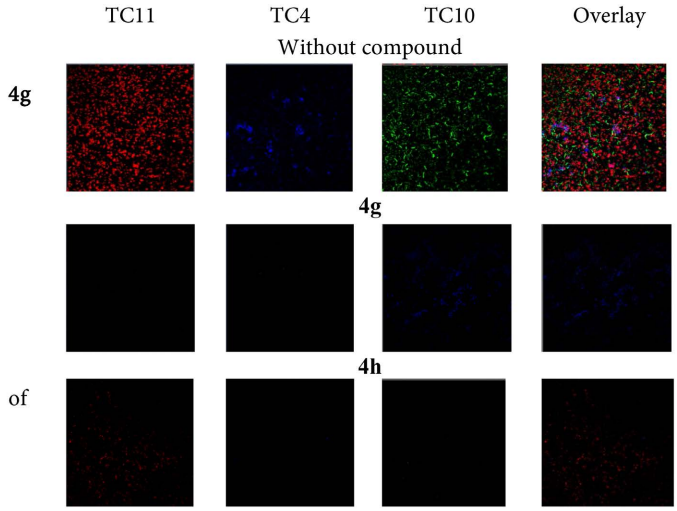

Figure 4. Confocal laser scanning microscopy images of the multispecies biofilm composed of *Persicivirga* (*Nonlabens*) *mediterranea* TC4, *Shewanella* sp. TC10, and *Shewanella* sp. TC11 on coverslips at 24 hours. Images show the biofilm without treatment as a reference (up) and treated with 100 µM of compound 4g (middle) and 4h (down). Images of each strain have been extracted, and the overlay of the three strains is shown on the right.

4. Conclusion

In summary, we have used click chemistry to investigate the chemical diversity of a library of hemibastadin analogues based on a triazole-amide framework. In the present paper, we have designed new analogues active against biofilm growth of gram-negative bacteria. Finally, the low toxicity of the more potent anti-biofilm leads allows us to focus on future interest in the development of these molecules as non-toxic anti-biofilm compounds for their potential use as non-toxic co-biocide or co-antibiotic in view of rational eradication of persistent biofilms.

Acknowledgements

We are especially grateful to the LBCM laboratory (Université de Bretagne Sud).

Conflicts of Interest

The authors declare no conflicts of interest regarding the publication of this paper.

References

[1] Yebra, D.M., Kiil, S. and Dam-Johansen, K. (2004) Antifouling Technology—Past, Present and Future Steps Towards Efficient and Environmentally Friendly Antifouling

Coatings. *Progress in Organic Coatings*, **50**, 75-104. https://doi.org/10.1016/j.porgcoat.2003.06.001

[2] Fitridge, I., Dempster, T., Guenther, J. and de Nys, R. (2012) The Impact and Control of Biofouling in Marine Aquaculture: A Review. *Biofouling*, **28**, 649-669. https://doi.org/10.1080/08927014.2012.700478

[3] Qian, P., Lau, S.C.K., Dahms, H., Dobretsov, S. and Harder, T. (2007) Marine Biofilms as Mediators of Colonization by Marine Macroorganisms: Implications for Antifouling and Aquaculture. *Marine Biotechnology*, **9**, 399-410. https://doi.org/10.1007/s10126-007-9001-9

[4] Müller, W.E.G., Brümmer, F., Batel, R., Müller, I.M. and Schröder, H.C. (2003) Molecular Biodiversity. Case Study: Porifera (Sponges). *Naturwissenschaften*, **90**, 103-120. https://doi.org/10.1007/s00114-003-0407-6

[5] Hamann, M.T., Scheuer, P.J. and Kelly-Borges, M. (1993) Biogenetically Diverse, Bioactive Constituents of a Sponge, Order Verongida: Bromotyramines and Sesquiterpene-Shikimate Derived Metabolites. *The Journal of Organic Chemistry*, **58**, 6565-6569. https://doi.org/10.1021/jo00076a012

[6] Krug, P.J. (2006) Defense of Benthic Invertebrates against Surface Colonization by Larvae: A Chemical Arms Race. In: Fusetani, N. and Clare, A.S., Eds., Antifouling Compounds, Springer-Verlag, 1-53. https://doi.org/10.1007/3-5403-0016-3_1

[7] Steinberg, P.D., Schneider, R. and Kjelleberg, S. (1997) Chemical Defenses of Seaweeds against Microbial Colonization. *Biodegradation*, **8**, 211-220. https://doi.org/10.1023/a:1008236901790

[8] Sun, J., Wu, J., An, B., Voogd, N., Cheng, W. and Lin, W. (2018) Bromopyrrole Alkaloids with the Inhibitory Effects against the Biofilm Formation of Gram Negative Bacteria. *Marine Drugs*, **16**, Article 9. https://doi.org/10.3390/md16010009

[9] Bhadury, P. and Wright, P. (2004) Exploitation of Marine Algae: Biogenic Compounds for Potential Antifouling Applications. *Planta*, **219**, 561-578. https://doi.org/10.1007/s00425-004-1307-5

[10] de Nys, R. and Steinberg, P.D. (2002) Linking Marine Biology and Biotechnology. *Current Opinion in Biotechnology*, **13**, 244-248. https://doi.org/10.1016/s0958-1669(02)00311-7

[11] Fusetani, N. (2004) Biofouling and Antifouling. *Natural Product Reports*, **21**, 94-104. https://doi.org/10.1039/b302231p

[12] Fusetani, N. (2011) Antifouling Marine Natural Products. *Natural Product Reports*, **28**, 400-410. https://doi.org/10.1039/c0np00034e

[13] Gerwick, W.H. and Moore, B.S. (2012) Lessons from the Past and Charting the Future of Marine Natural Products Drug Discovery and Chemical Biology. *Chemistry & Biology*, **19**, 85-98. https://doi.org/10.1016/j.chembiol.2011.12.014

[14] Hellio, C., Tsoukatou, M., Maréchal, J., Aldred, N., Beaupoil, C., Clare, A.S., *et al.* (2005) Inhibitory Effects of Mediterranean Sponge Extracts and Metabolites on Larval Settlement of the Barnacle Balanus Amphitrite. *Marine Biotechnology*, **7**, 297-305. https://doi.org/10.1007/s10126-004-3150-x

[15] Maréchal, J. and Hellio, C. (2009) Challenges for the Development of New Non-Toxic Antifouling Solutions. *International Journal of Molecular Sciences*, **10**, 4623-4637. https://doi.org/10.3390/ijms10114623

[16] Sipkema, D., Franssen, M.C.R., Osinga, R., Tramper, J. and Wijffels, R.H. (2005) Marine Sponges as Pharmacy. *Marine Biotechnology*, **7**, 142-162. https://doi.org/10.1007/s10126-004-0405-5

[17] Stowe, S.D., Richards, J.J., Tucker, A.T., Thompson, R., Melander, C. and Cavanagh,

J. (2011) Anti-Biofilm Compounds Derived from Marine Sponges. *Marine Drugs*, **9**, 2010-2035. https://doi.org/10.3390/md9102010

[18] Tsukamoto, S., Kato, H., Hirota, H. and Fusetani, N. (1996) Ceratinamides A and B: New Antifouling Dibromotyrosine Derivatives from the Marine Sponge Pseudoceratina Purpurea. *Tetrahedron*, **52**, 8181-8186. https://doi.org/10.1016/0040-4020(96)00387-0

[19] Tornøe, C.W., Charistensen, C. and Meldal, M. (2002) Peptidotriazoles on Solid Phase: [1,2,3]-Triazoles by Regiospecific Copper(I)-Catalyzed 1,3-Dipolar Cycloadditions of Terminal Alkynes to Azides. *The Journal of Organic Chemistry*, **67**, 3057-3064.

[20] Andjouh, S. and Blache, Y. (2015) Click-Based Synthesis of Bromotyrosine Alkaloid Analogs as Potential Anti-Biofilm Leads for SAR Studies. *Bioorganic & Medicinal Chemistry Letters*, **25**, 5762-5766. https://doi.org/10.1016/j.bmcl.2015.10.073

[21] Andjouh, S. and Blache, Y. (2016) Screening of Bromotyramine Analogues as Antifouling Compounds against Marine Bacteria. *Biofouling*, **32**, 871-881. https://doi.org/10.1080/08927014.2016.1200562

[22] Rostovtsev, V.V., Green, L.G., Fokin, V.V. and Sharpless, K.B. (2002) A Stepwise Huisgen Cycloaddition Process: Copper(I)-Catalyzed Regioselective "Ligation" of Azides and Terminal Alkynes. *Angewandte Chemie International Edition*, **41**, 2596-2599. https://doi.org/10.1002/1521-3773(20020715)41:14<2596::aid-anie2596>3.0.co;2-4

[23] Brian-Jaisson, F., Ortalo-Magné, A., Guentas-Dombrowsky, L., Armougom, F., Blache, Y. and Molmeret, M. (2014) Identification of Bacterial Strains Isolated from the Mediterranean Sea Exhibiting Different Abilities of Biofilm Formation. *Microbial Ecology*, **68**, 94-110. https://doi.org/10.1007/s00248-013-0342-9

[24] Grasland, B., Mitalane, J., Briandet, R., Quemener, E., Meylheuc, T., Linossier, I. and Haras, D. (2003) Bacterial Biofilm in Seawater: Cell Surface Properties of Early-Attached Marine Bacteria. *Biofouling*, **19**, 307-313. https://doi.org/10.1080/0892701031000121041

[25] Camps, M., Briand, J., Guentas-Dombrowsky, L., Culioli, G., Bazire, A. and Blache, Y. (2011) Antifouling Activity of Commercial Biocides Vs. Natural and Natural-Derived Products Assessed by Marine Bacteria Adhesion Bioassay. *Marine Pollution Bulletin*, **62**, 1032-1040. https://doi.org/10.1016/j.marpolbul.2011.02.031

[26] Leroy, C., Delbarre-Ladrat, C., Ghillebaert, F., Rochet, M.J., Compère, C. and Combes, D. (2007) A Marine Bacterial Adhesion Microplate Test Using the DAPI Fluorescent Dye: A New Method to Screen Antifouling Agents. *Letters in Applied Microbiology*, **44**, 372-378. https://doi.org/10.1111/j.1472-765x.2006.02103.x

[27] Guillonneau, R., Baraquet, C., Bazire, A. and Molmeret, M. (2018) Multispecies Biofilm Development of Marine Bacteria Implies Complex Relationships through Competition and Synergy and Modification of Matrix Components. *Frontiers in Microbiology*, **9**, Article 1960. https://doi.org/10.3389/fmicb.2018.01960

[28] Kacou, A., Ouvrard, A., Jamet, D., Jamet, J. and Blache, Y. (2019) Towards Ecofriendly Biocides: Preparation, Antibiofilm Activity of Hemibastadin Analogues. *Letters in Applied Microbiology*, **68**, 360-368. https://doi.org/10.1111/lam.13150

[29] Heydorn, A., Nielsen, A.T., Hentzer, M., Sternberg, C., Givskov, M., Ersbol, B.K. and Molin, S. (2000) Quantification of Biofilm Structures by the Novel Computer Program Comstat. *Microbiology*, **146**, 2395-2407. https://doi.org/10.1099/00221287-146-10-2395

[30] Vorregaard, M. (2008) Comstat2—A Modern 3D Image Analysis Environment for Biofilms, 85.